UNITED STATES DEPARTMENT OF THE INTERIOR

GEOLOGICAL SURVEY

FLUID IMPACT CRATERS AND HYPERVELOCITY--HIGH-VELOCITY IMPACT EXPERIMENTS IN METALS AND ROCKS

by

H. J. Moore, R. W. MacCormack, and

D. E. Gault

May 1963

Open File Report

This report concerns work done on behalf of the National Aeronautics and Space Administration

UNITED STATES DEPARTMENT OF THE INTERIOR

GEOLOGICAL SURVEY

FLUID IMPACT CRATERS AND HYPERVELOCITY--HIGH-VELOCITY IMPACT EXPERIMENTS IN METALS AND ROCKS

by

H. J. Moore, R. W. MacCormack[1/], and

D. E. Gault[1/]

May 1963

Open File Report

This report concerns work done on behalf of the National Aeronautics and Space Administration

This preliminary report is released without editorial and technical review for conformity with official standards and nomenclature.

1/ Ames Research Center, National Aeronautics and Space Administration, Moffett Field, California.

Contents

Illustrations

Table 1

FLUID IMPACT CRATERS AND HYPERVELOCITY--HIGH-VELOCITY IMPACT EXPERIMENTS IN METALS AND ROCKS

By H. J. Moore, R. W. MacCormack[1/], and D. E. Gault[1/]

Introduction

The impact phenomena of hypervelocity and high-velocity projectiles with rock and metal targets are being studied in a cooperative research program conducted by the U.S. Geological Survey and the Ames Research Center of the National Aeronautics and Space Administration. This paper deals with the comparison of: (1) fluid-impact craters produced by water drops impacting water, (2) hypervelocity and high-velocity impact craters produced by impact of steel, aluminum, and polyethylene projectiles with basalt, and (3) hypervelocity and high-velocity impact craters in metals.

The theoretical formula of Charters and Summers (1959) has been tested in this investigation and found approximately valid for impact of water drops into water. In addition, the formula indicates that deformation strengths of metals and rocks are placed at some value between a maximum deformation strength of the target material and its compressive strength at low confining pressures. The maximum deformation strength is the product of the heat of fusion and the density of the target material. The use of shear strengths and densities of the metal and rock-target materials

---

1/ National Aeronautics and Space Administration, Ames Research Center, Moffett Field, California.

at 49 kilobars for parameters yields fair agreement between (1) the theory of Charters and Summers, (2) experiments with cratering by water drops impacting water, and (3) hypervelocity impact experiments in and near the fluid-impact regime using rock and metal targets.

The study has concluded that shear strength or compressive strength of the target material is a more realistic parameter than acoustic velocity. When acoustic velocity is used as a parameter, water-drop cratering experiments cannot be correlated with theory or with experimental data on high-velocity to hypervelocity impact cratering in rocks and metals.

Cratering theory of Charters and Summers

A quantitative theory for craters produced by projectile impact in the fluid-impact regime has been proposed by Charters and Summers (1959). In their theory, the momentum or, more precisely, the product of the mass and speed of a uniformly expanding hemispherical shell composed of both the projectile and the target material is assumed to be equal to the projectile momentum

$$m_{fs}\mu_{fs} = m_p V_p \tag{1}$$

where

m_{fs} = mass of fluid shell,

μ_{fs} = velocity of fluid shell,

m_p = mass of projectile,

V_p = velocity of projectile.

The kinetic energy of the projectile is then compared to the kinetic energy of the fluid shell using the hydraulic analogy of the shaped charge penetration for which

$$\mu_{fs} = \frac{1}{2} V_p \tag{2}$$

then

$$m_{fs}\mu^2_{fs} = \frac{1}{2} m_p V^2_p . \tag{3}$$

The kinetic energy of the fluid shell is assumed to be used in the work of deformation in forming the crater:

$$\frac{1}{2} m_{fs}\mu^2_{fs} = \int_0^p S\, 2\pi r^2\, dr \tag{4}$$

where

S = the deformation strength,

p = the maximum crater depth,

r = the radius of the hemispherical crater cavity.

Integration, when S is constant, gives

$$\frac{1}{2} m_{fs} \mu^2_{fs} = \frac{2}{3} \pi p^3 S \tag{5}$$

and since

$$m_{fs} \mu^2_{fs} = \frac{1}{2} m_p V^2_p \tag{6}$$

then

$$m_p V^2_p = \frac{8}{3} \pi p^3 S \tag{7}$$

or

$$S = \frac{3 m_p V^2_p}{8 \pi p^3}. \tag{8}$$

Then, taking into account experimental data and rearranging terms, the penetration formula becomes

$$\frac{p}{d} = \frac{1}{2} \left(\frac{\rho_p}{\rho_t} \right)^{1/3} \left(\frac{\rho_p V^2_p}{2S} \right)^{1/3} \tag{9}$$

which can be rewritten

$$S = \frac{1}{16} \frac{\rho_p^2}{\rho_t} \frac{V^2_p}{\left(\frac{p}{d}\right)^3}$$

where

d = diameter of the projectile,

ρ_p = density of the projectile,

ρ_t = density of the target.

Engel's water craters

Preliminary studies of craters produced by water drops impacting water (Engel, 1961) yield data that permit a quantitative test of the fluid-impact theory of Charters and Summers. The water-drop experiments employed projectiles of 11 mg, 56 mg, and 183 mg which impacted water with velocities of 400 to 700 cm/sec. The experiments of Engel produced temporary craters from 7.25 mm to 21.9 mm in depth. In addition, Engel points out many similarities between the water-drop experiments and some hypervelocity impact experiments.

Deformation strengths of the water for each experiment can be calculated in two ways: (1) by employing a knowledge of the physical properties of water and the experimental measurements, and (2) by employing the theory of Charters and Summers.

Three types of resistance oppose the process of crater formation in water: (1) the hydrostatic pressure head, (2) surface tension, and (3) the resistance of the water to flow (or viscosity). The deformation strength then becomes

$$S_w = f(\rho_w g z) + f\left(\frac{2\gamma}{z}\right) + f\left(\frac{V_t \mu}{x}\right) \qquad (10)$$

where

S_w = deformation strength of water,

ρ_w = density of water,

g = acceleration of gravity,

z = a depth or vertical coordinate,

$\frac{V_t}{x}$ = a velocity gradient,

μ = viscosity of water (10^{-2} dynes-sec/cm^2),

γ = surface tension of water (72 dynes/cm).

During the cratering process in water, the deformation strength related to the hydrostatic pressure head increases from zero to some finite value, since z increases from zero to p or the maximum crater depth. The effective deformation strength resulting from the hydrostatic pressure head may be obtained by computing the work required to form a crater against the hydrostatic pressure head and relating this to the final crater volume. The work required to form a hemispherical crater against the hydrostatic pressure head may be expressed

$$W_{hh} = \int_0^F dF\ z = \int_0^{Vol} \rho_w g\ d(Vol)z \qquad (11)$$

where

W_{hh} = work expended in overcoming hydrostatic pressure head,

dF = incremental force on an incremental volume of water removed from crater to surface of water,

p = maximum crater depth of hemispherical crater,

ρ_w = density of water,

g = acceleration of gravity,

z = depth or vertical coordinate,

d(Vol) = an incremental volume of water removed from crater to surface of water.

Integration of equation (11) yields

$$W_{hh} = \frac{\pi \rho g p^4}{4} . \qquad (12)$$

If the mean or effective deformation strength due to the hydrostatic pressure head is defined by S_{hh}, then

$$W_{hh} = S_{hh} \int_0^p 2\pi r^2 \, dr \tag{13}$$

and

$$S_{hh} = \frac{3\rho_w g p}{8} . \tag{14}$$

The mean or effective deformation strength due to surface tension may be derived in a similar manner. The work required to overcome surface tension is

$$W_{st} = \int_0^{2\pi p^2} \gamma \, dA \tag{15}$$

where

W_{st} = work expended in overcoming surface tension,

γ = surface tension of water,

dA = change in area,

p = maximum crater depth of hemispherical crater.

Then

$$W_{st} = 2\pi \gamma p^2 \tag{16}$$

and

$$W_{st} = S_{st} \int_0^p 2\pi r^2 \, dr \tag{17}$$

where

S_{st} = effective or mean deformation strength due to surface tension

or

$$S_{st} = \frac{3\gamma}{p} . \tag{18}$$

Approximate values for the deformation strength of the water due to viscosity during the cratering process may be obtained by assuming that the flow of the projectile and target material occurs near the projectile-target interface. In addition, the flow is assumed to occur within a layer twice as thick as the projectile smeared evenly over a hemispherical crater at maximum depth. Also, it may be assumed that the velocities of

the flow are approximately equal to the radial velocities of the fluid shell. The estimated deformation strength due to viscosity then becomes

$$S_{\mu} = f\left(\frac{V_t}{x}\,\mu\right) = \mu\,\frac{1}{t}\int_0^t \frac{\dfrac{d(z)}{dt}}{\dfrac{2\,vol_p}{2\pi p^3}}\,dt \qquad (19)$$

where

S_{μ} = deformation strength due to viscosity,

μ = viscosity of water $\left(\dfrac{10^{-2}\text{dynes-sec}}{\text{cm}^2}\right)$,

t = duration of cratering event,

$\dfrac{d(z)}{dt}$ = radial velocity of fluid shell,

vol_p = volume of projectile,

p = maximum crater depth,

$\dfrac{V_t}{x}$ = velocity gradient.

Equation 19 can be evaluated using the data of Engel (1961).

The calculated deformation strengths for the individual experiments of water impacting water (Engel, 1961) using the effective deformation strengths due to hydrostatic pressure head, surface tension, and estimated strength due to viscosity, and assuming hemispherical craters are tabulated (table 1).

Deformation strengths for the water craters, assuming spherical projectiles and hemispherical craters, have been calculated using the Charters-Summers theory (equation 9). These deformation strengths are listed in table 1, column 5. In addition, the data are plotted in figure 1, where p is the maximum crater depth.

The assumption of hemispherical water craters which are actually prolate hemispheroids leads to minor errors, so that the calculations

represent approximate values for the mean or effective deformation strength of the water craters. The correct values for the mean or effective deformation strength of the water during cratering are very near $\frac{1 \times 10^3 \text{dynes}}{\text{cm}^2}$.

Table 1. Computed deformation strengths of water for craters produced by impact of water drops into water.

Experiment (Engel 1961)	(1) Hydrostatic pressure head (Equation 14) $\frac{3}{8}\rho_w g p$ (dynes/cm^2)	(2) Surface tension (Equation 18) $\frac{3\gamma}{p}$ (dynes/cm^2)	(3) Estimated strength due to viscosity (Equation 19) $f\left(\frac{V_t}{x}\mu\right)$ (dynes/cm^2)	(4) Total deformation strength (Equation 10) S_w (dynes/cm^2)	(5) Deformation strength calculated with Charters-Summers theory (Equation 9) $\frac{1}{16}\frac{\rho_p^2}{\rho_t}\frac{V_p^2}{(p/d)^3}$ (dynes/cm^2)
11-400	0.27×10^3	0.30×10^3	0.07×10^3	0.64×10^3	0.57×10^3
11-650	0.36×10^3	0.22×10^3	0.13×10^3	0.71×10^3	0.61×10^3
56-400	0.44×10^3	0.18×10^3	0.03×10^3	0.65×10^3	0.62×10^3
56-700	0.53×10^3	0.15×10^3	0.08×10^3	0.76×10^3	1.07×10^3
182-400	0.62×10^3	0.13×10^3	0.03×10^3	0.78×10^3	0.73×10^3
182-700	0.80×10^3	0.10×10^3	0.07×10^3	0.97×10^3	0.98×10^3

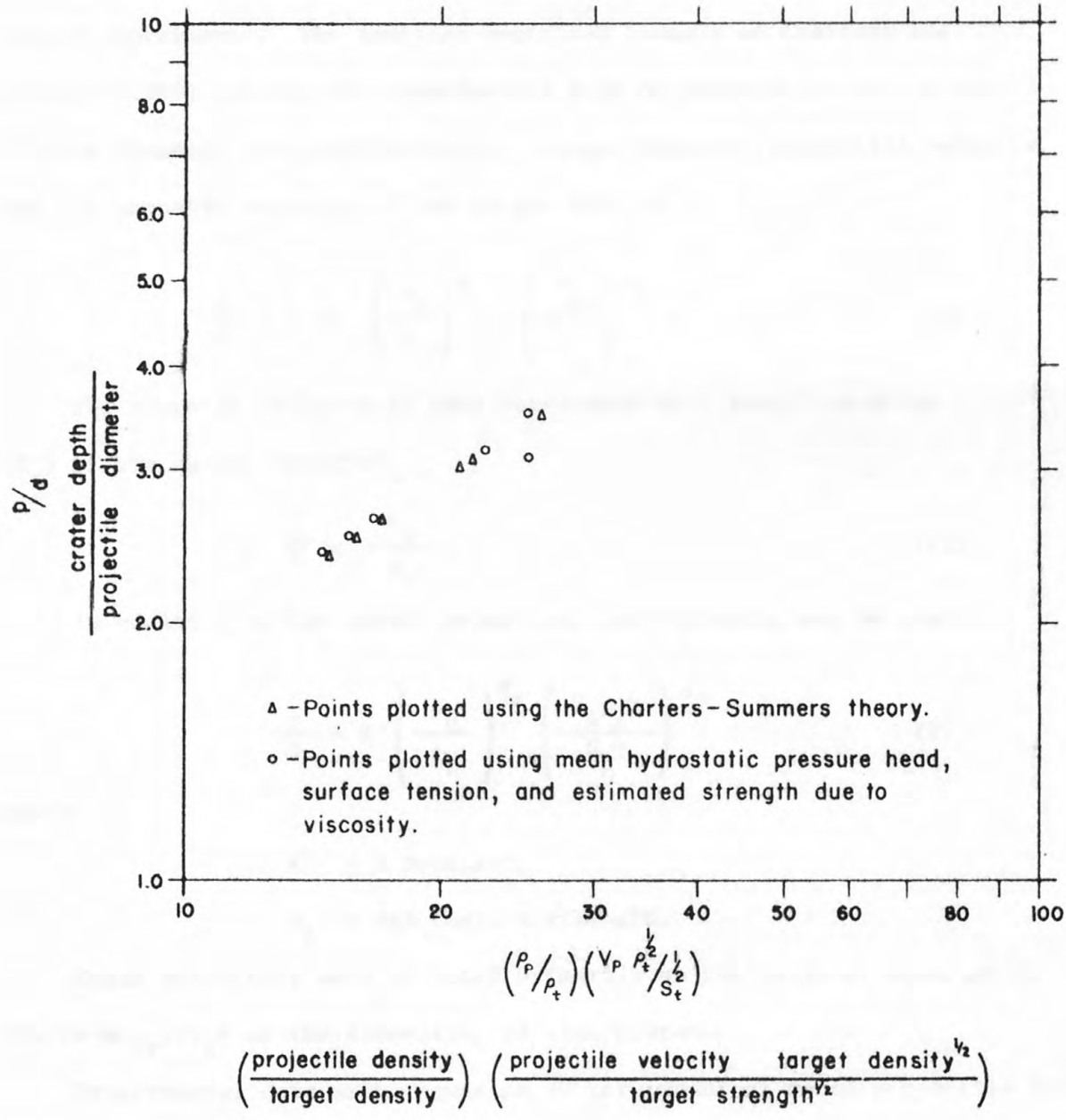

Figure 1. Graph comparing deformation strength of water computed by using the mean hydrostatic pressure head, surface tension and estimated strength due to viscosity, and the theory of Charters-Summers.

Parameters

Various parameters have been used to correlate hypervelocity fluid-impact experiments. The familiar empirical formula of Charters and Summers (1959) relates the experimental data on penetration to the projectile diameter, projectile density, target density, projectile velocity, and the acoustic velocity of the target material:

$$\frac{p}{d} = 2.28 \left(\frac{\rho_p}{\rho_t}\right)^{2/3} \left(\frac{V_p}{C}\right)^{2/3} . \tag{20}$$

The acoustic velocity is then correlated with Young's modulus (E_t) of the target material:

$$C^2 = \frac{E_t}{\rho_t} . \tag{21}$$

In addition to the above parameters, the following may be used:

$$\frac{p}{d} = K \left(\frac{\rho_p}{\rho_t}\right)^{2/3} \left(\frac{V_p \rho_t^{1/2}}{S_t^{1/2}}\right)^{2/3} \tag{22}$$

where

K = a constant,

S_t = deformation strength.

These parameters were selected primarily on the basis of equation 9. The term $\rho_t^{1/2}/S_t^{1/2}$ as the dimensions of time/distance.

Experimental data using equation 22 for impact of metal projectile into metal, metal projectile into rock, and water projectile into water are shown in figure 2. In addition, a plot using the reciprocal of the square root of the heat of fusion in place of $\rho_t^{1/2}/S_t^{1/2}$ has been included in figure 2. This parameter, which has been suggested by Whipple (1958) and Bromberg (in Palmer and others, 1960, p. 8), also has the dimensions of time/distance.

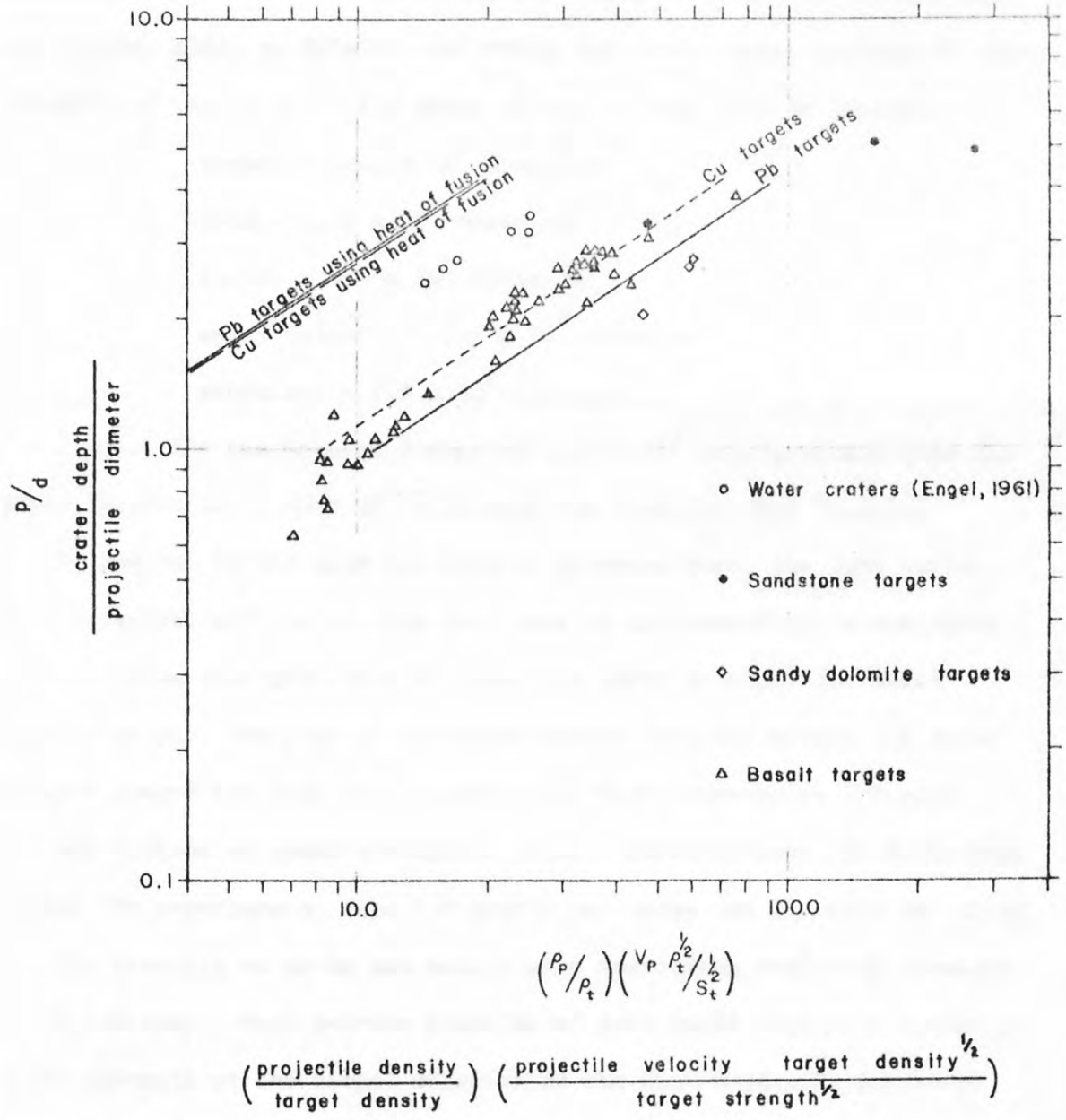

Figure 2. Graph comparing craters produced by impact of water drops into water, metal spheres impacting copper and lead targets, and metal and polyethylene spheres impacting rocks using $\rho_t^{\frac{1}{2}}/S_t^{\frac{1}{2}}$ as measured at normal confining pressures. A plot for copper and lead cratering experiments using the reciprocal of the square root of the target heat of fusion in place of $\rho_t^{\frac{1}{2}}/S_t^{\frac{1}{2}}$ is included.

Figure 2 is based on experimental data for impacts using rock targets; information from Moore and Gault (1963), Summers (1959), the Metals Handbook (Lyman, 1958, p. 905-909, 961-962); and actual determination of shear strengths of the rocks. The shear strengths used were as follows:

copper - 1.53×10^9 dynes/cm^2

lead - 1.26×10^8 dynes/cm^2

basalt - 8.6×10^8 dynes/cm^2

sandy dolomite - 2.8×10^8 dynes/cm^2

sandstone - 1.9×10^8 dynes/cm^2.

A value for the heat of fusion of 2.12×10^9 ergs/gram was used for copper targets and 2.62×10^8 ergs/gram was used for lead targets.

If the sum of the mean hydrostatic pressure head, the mean surface tension factor, and the viscous head loss is considered to be analogous to compressive strength which is twice the shear strength for ideal plastic failure, the plot of the experimental data for metals and rocks is moved toward the left by a factor of $\sqrt{2}$ when compressive strengths are used instead of shear strengths. Such a shift reduces the difference between the experimental data for metals and rocks and the data for water.

The strength of rocks and metals with increasing confining pressure is not constant. More precise plotting of data would require a knowledge of the strength of the target material at the high confining pressures which are produced during crater formation by impact of hypervelocity projectiles. The maximum strength of the target may be taken as the product of the heat of fusion and density of the target material, and the minimum strength as the compressive strength at low confining pressures. The deformation strength during cratering by hypervelocity and high-velocity impacts would lie between these two values.

Strengths and densities at high confining pressures

A good deal is known about the density of some materials up to 700 kilobars confining pressure, and in some cases up to several megabars (Rice and others, 1958, Al'tshuler and others, 1960). Little is known about the strength of materials above 49 kilobars. However, the existing data on the strengths and densities of metals and rocks may be used to illustrate how correlation of impact-cratering experiments could be improved by the parameter $\rho_t^{\frac{1}{2}}/S_t^{\frac{1}{2}}$ and the plot of cratering experiments in and near the fluid-impact regime.

The plots of hypervelocity-impact data for copper and lead in and near the fluid-impact regime indicate that $\rho_t^{\frac{1}{2}}/S_t^{\frac{1}{2}}$ is constant because of the constant slope of $\frac{2}{3}$ (Summers, 1959). If it is further assumed that $\rho_t^{\frac{1}{2}}/S_t^{\frac{1}{2}}$ for metals becomes constant at and above 49 kilobars and that ρ_p/ρ_t is essentially constant, the shear strength and density at 49 kilobars (Bridgman, 1935; Rice and others, 1958) may be used to evaluate $\rho_t^{\frac{1}{2}}/S_t^{\frac{1}{2}}$ at high pressures.

The assumption that ρ_p/ρ_t is constant may be justified from compressibility data obtained with shock techniques. Compressibility ratios for copper, lead, aluminum, iron, and magnesium projectiles impacting copper and lead targets range between 0.850 and 1.065 at 100 kilobars and 0.850 and 1.174 at 500 kilobars. Thus the assumption of a constant ratio for ρ_p/ρ_t is valid within $\pm$ 10 percent at 100 kilobars and $\pm$ 16 percent at 500 kilobars. This range is within the scatter of experimental data for metals and rocks (see, for example, Charters and Summers, 1959; Summers, 1959, p. 13). The shear strengths for lead and copper at 49 kilobars are 710 kg/cm^2 (6.96×10^8 dynes/cm^2) and 4700 kg/cm^2 (4.6×10^9 dynes /cm^2)

(Bridgman, 1935). The densities of lead and copper which were obtained by extrapolation of densities obtained with shock-wave techniques (Rice and others, 1958) and static compression techniques (Bridgman, 1935) are 12.4 grams/cm^3 and 9.35 grams/cm^3 at 49 kilobars.

The use of the shear strengths and densities at 49 kilobars confining pressure yields good results (compare fig. 3). Impact data for lead and copper are practically coincident at this pressure, whereas at low confining pressures they vary. In addition, craters produced by water drops impacting water agree more closely with craters produced by metal projectiles impacting metal targets near the fluid-impact regime.

Similar data are available for some rocks. There are no data on basalt for shear strengths at 49 kilobars. However, 15.5 x 10^9 dynes/cm^2 for the strength of basalt at high confining pressures can be estimated by comparing the shear strength of basalt glass, which is 17.0 x 10^9 dynes/cm^2, and pyroxenite, which is 14.0 x 10^9 dynes/cm^2 (Bridgman, in Robertson, 1955). This estimate is justified by generalizations of shear strengths of rocks which tend to be approximately the same at high confining pressures (Robertson, 1955). The density of basalt at 49 kilobars may be estimated with data from shock-wave techniques (Lombard, 1961). Such an estimate yields 2.9 to 3.0 grams/cm^3.

The data plotted in figure 3 for basalt fall to the left of those for the metals and water, confirming that the cratering process in rocks differs from that in metals and water. This difference is due to the low tensile strength of rocks at low confining pressures. For craters of the size produced in the laboratory experiments, a projectile that has impacted rock is ejected completely from the crater along with rock debris, whereas one that has impacted metal smears out and plates the crater floor and

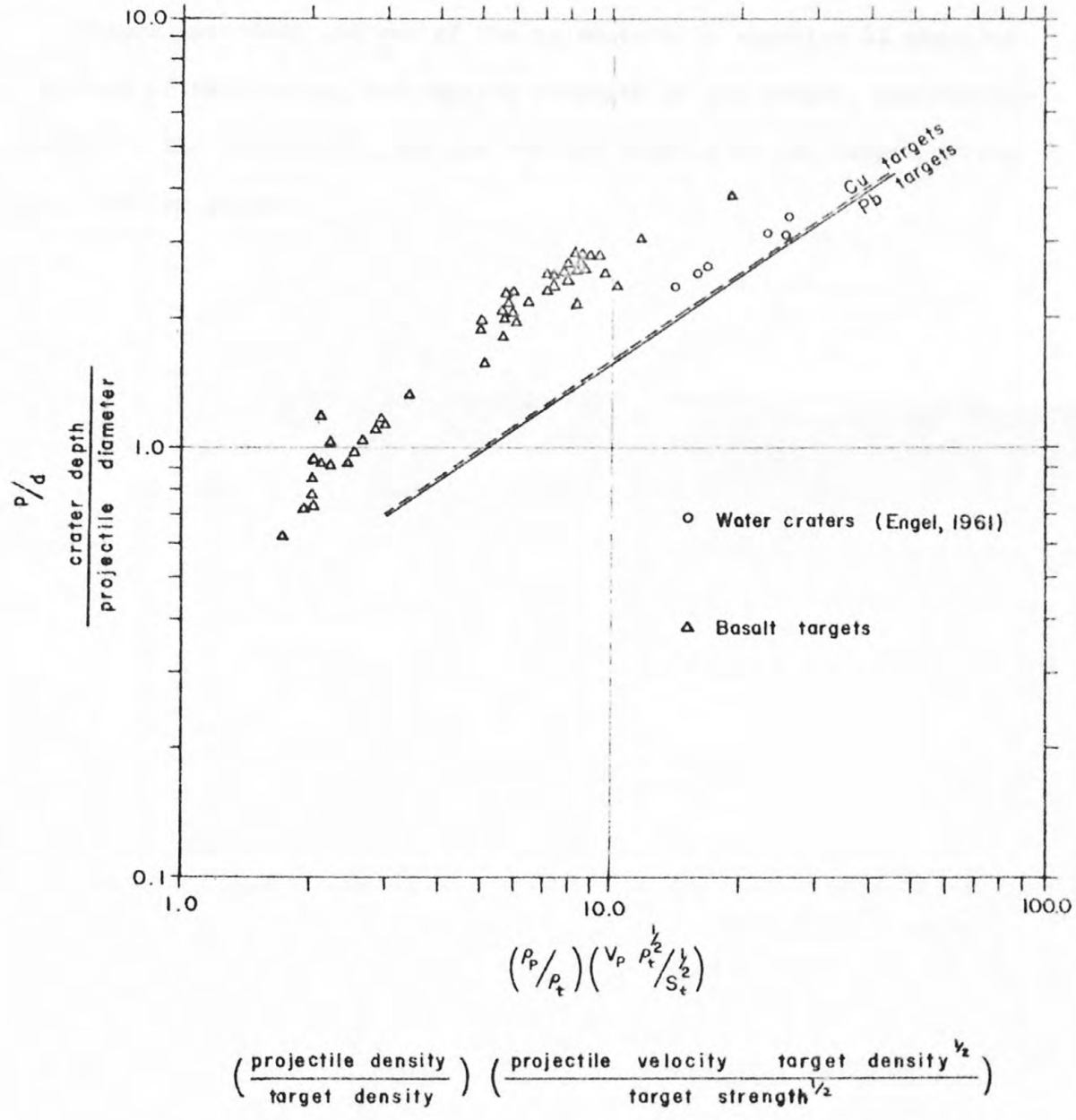

Figure 3. Graph comparing craters produced by impact of water drops into water, metal spheres impacting copper and lead targets, and metal and polyethylene sphere impacting basalt using $\rho_t^{1/2}/S_t^{1/2}$ as estimated for 49 kilobars confining pressure.

walls (Summers, 1959). Plating also occurs in craters produced by water-drop impacts with water (Engel, 1961; Charters, 1960).

Proper appraisal and use of the parameters in equation 22 requires knowledge of the average deformation strength of the target, the average density of the projectile, and the average density of the target during the cratering process.

Acoustic velocity as a parameter

The primary problem with acoustic velocity as a parameter is shown clearly in the case of fluid impacts of water into water. The use of the acoustic velocity of water (which is 1.5 km/sec) in Engel's experiments did not permit plotting of the fluid-impact water-drop experiments and the fluid-impact metal and rock experiments in the same decade on log-log paper. The use of either shear or compressive strength at either low or high confining pressure, divided by [redacted] the target density or the target heat of fusion, does permit such a plot.

Crater volume-energy relationships

The relationships between crater volume and the energy of the devices producing the craters further illustrates the effects of the properties of the target material (see fig. 4). For example, in figure 4 the volumes of hypervelocity impact craters in copper are almost one order of magnitude smaller than hypervelocity impact craters in lead although the projectile energies are about the same (Summers and Nysmith, 1962, oral and written communications). The volumes of hypervelocity impact craters produced in aluminum by hypervelocity aluminum projectiles with energies comparable to the projectiles used for the lead and copper experiments would be smaller than the volumes of the craters in lead but larger than the volumes of the craters in copper (Halperson and Atkins, 1962). The yields for the copper, lead, and aluminum hypervelocity impact craters range between about 5×10^{-11} cm^3/erg and 5×10^{-10} cm^3/erg. Temporary water craters with volumes comparable to the craters in metals are produced by water impacting water with energies seven to eight orders of magnitude less than the energies of the metal projectiles used in producing the craters in metals. Yields for the temporary water craters are about 10^{-3} cm^3/erg. In addition, craters in paraffin wax produced by paraffin wax projectiles yield about 2.4×10^{-9} cm^3/erg (Palmer and others, 1960). Hypervelocity impact craters in rocks show similar discrepancies. For example, the volumes of hypervelocity impact craters in basalt are almost two orders of magnitude smaller than the volume of a hypervelocity impact crater in diatomaceous earth, although the projectile energies are about the same.

In addition to the problems associated with the properties of the materials used in an experiment, there is a problem of the effects of the size of the cratering event or experiment. Because it has been suggested

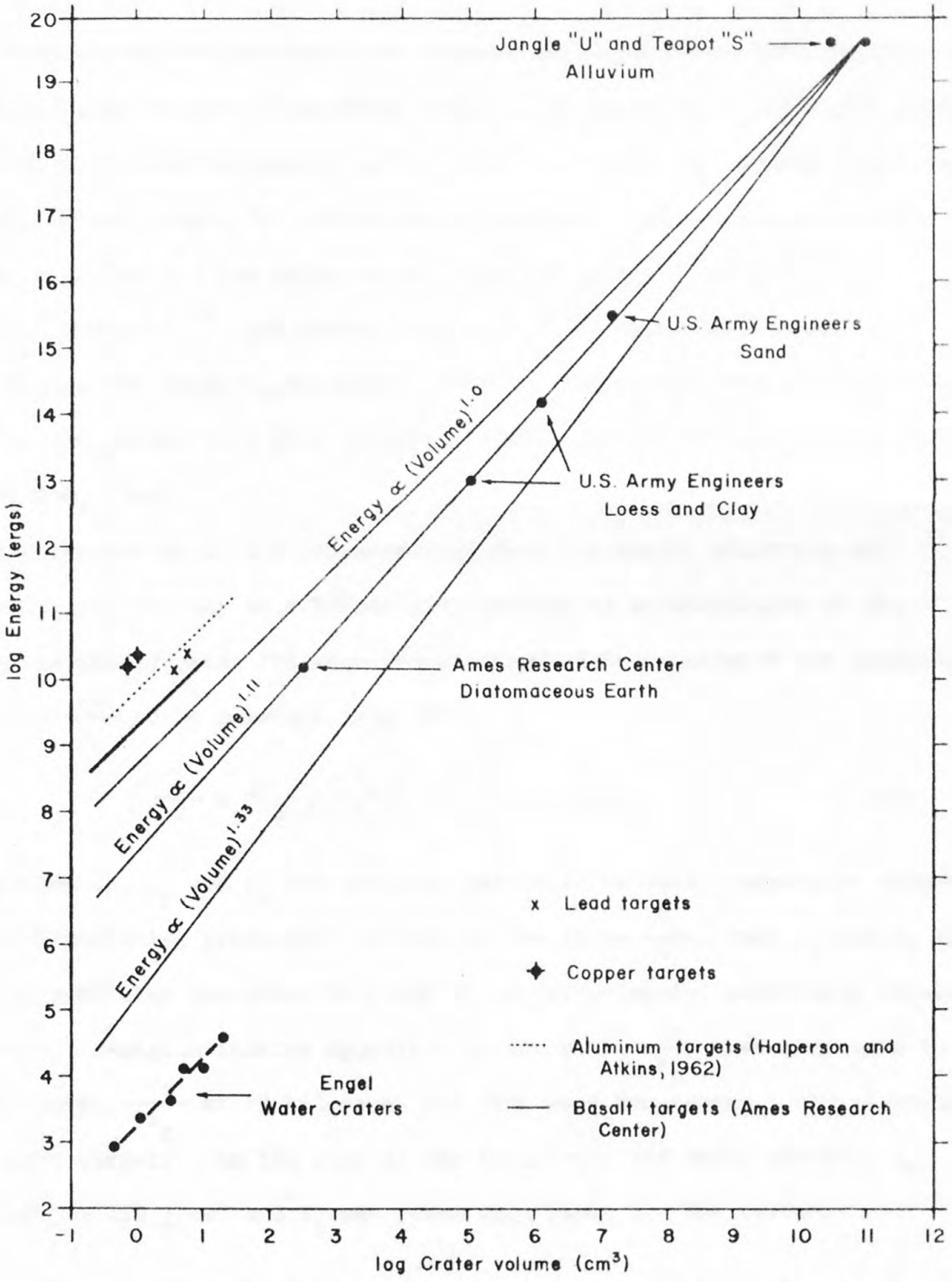

Figure 4. Comparison of crater volume-energy relationships between various cratering experiments.

that chemical and nuclear explosive craters might correlate with hypervelocity impact craters (Shoemaker, 1960), some cratering experiments using chemical (U.S. Army Engineers, sand, loess, and clay) and nuclear explosives (Jangle "U" and Teapot "S", alluvium) at shallow depths of burial are included in figure 4. The three lines, labelled energy $\propto$ (volume)$^{1.0}$, energy $\propto$ (volume)$^{1.11}$, and energy $\propto$ (volume)$^{1.33}$, represent Lampson's scaling (see for example, Shoemaker, 1960, p. 431), empirical scaling developed at the Nevada Test Site (Nordyke, 1962), and gravity scaling (Chabai and Hankins, 1960).

The separation of the volume-energy data for impact cratering experiments (fig. 4) may be substantially reduced by normalization of the projectile energy using the requirements imposed by equation 9 and assuming the ratio $\frac{\rho_p}{\rho_t}$ to be constant (fig. 5):

$$\left(\frac{1}{2} m_p V^2_p\right)\left(\frac{\rho_t}{S_t}\right)\left(\frac{\rho_p}{\rho_t}\right) \propto \mathrm{Vol}_t \rho_t. \qquad (23)$$

In equation 23, ρ_p and ρ_t are constant and equal to their respective values at normal confining pressures; whereas in the ratio $\frac{\rho_t}{S_t}$, both ρ_t and S_t at elevated confining pressures dictated by the experimental conditions should be used. A semiquantitative appraisal of the ratio $\frac{\rho_t}{S_t}$ has been used in figure 5 where $\frac{\rho_t}{S_t}$ at 49 kilobars has been used for copper, lead, aluminum, and basalt targets. In the case of the ratio $\frac{\rho_t}{S_t}$ for water craters, ρ_t was taken as 1.0 g/cm^3 and S_t was taken from table 1. The value of $\frac{\rho_t}{S_t}$ for the wax target was taken from data at 20 kilobars because the highest velocities used for wax experiments, which were 2 x 10^5 cm/sec, require a Bernoulli stagnation pressure near 20 kilobars (Palmer and others, 1960,

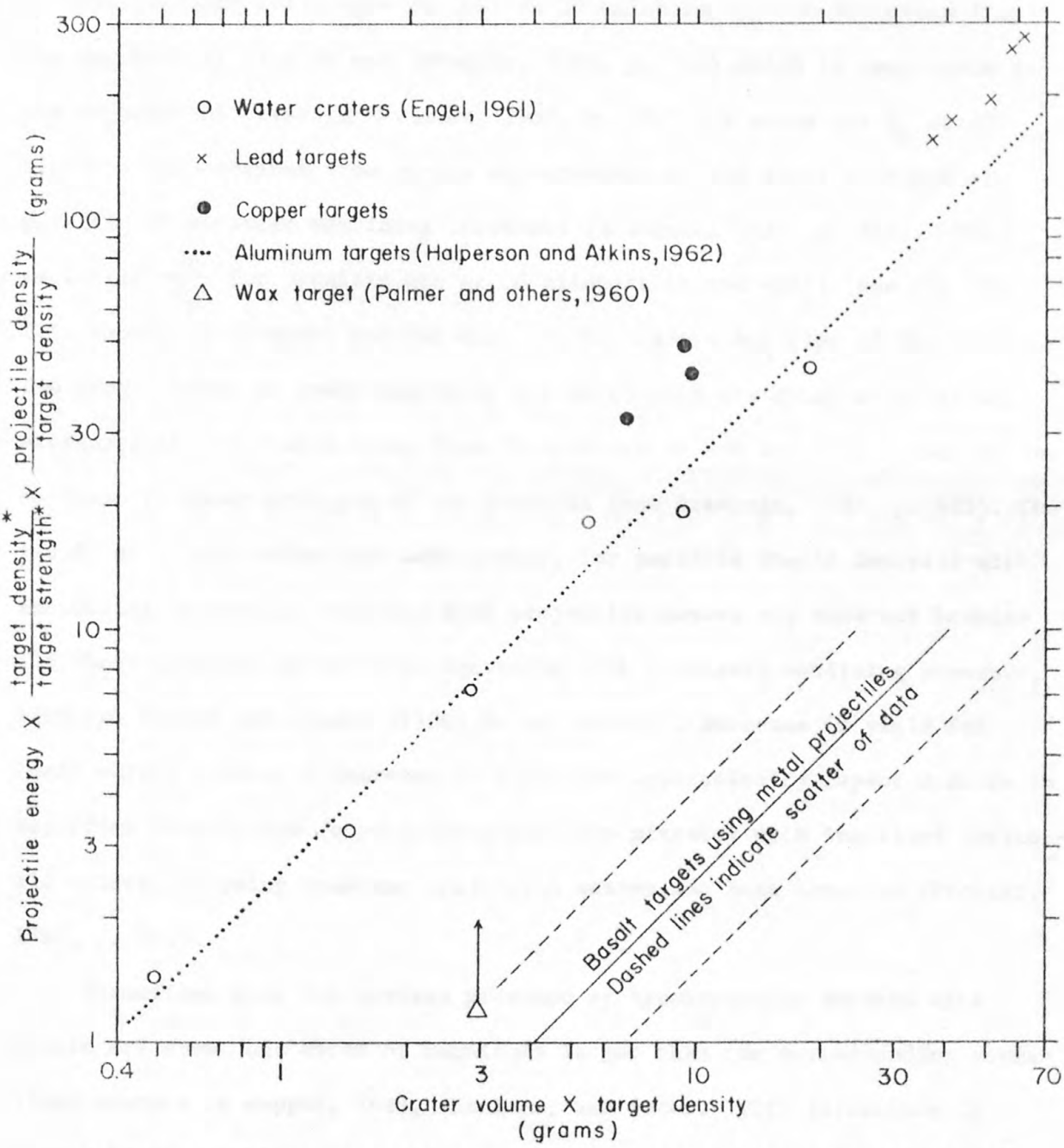

Figure 5. Normalized volume-energy data for impact cratering experiments using target strength, target density, and projectile density. Terms marked with asterisk from data measured at 49 kilobars confining pressure for lead, copper, aluminum and basalt, from data measured at 20 kilobars confining pressure for wax, and from table 1 for water craters.

p. 14). For the ratio $\frac{\rho_t}{S_t}$ for wax at 20 kilobars, ρ_t was estimated from the Hugoniot of plastic wax (Frasier, 1962, p. 384) which is comparable to the Hugoniot of paraffin (Frasier, 1962, p. 386). A value for S_t at 20 kilobars was obtained from static measurements of the shear strength of paraffin at elevated confining pressures (Bridgman, 1935, p. 833). The ratio for $\frac{\rho_t}{S_t}$ for paraffin wax at 20 kilobars is too small (see fig. 5). This should be expected because most of the failure and flow of the paraffin should occur at lower confining pressures with the decay of confining pressures in the stress waves from 20 kilobars to one bar with a concomitant decrease in shear strength of the paraffin (see Bridgman, 1935, p. 833). The yield, or crater volume per unit energy, for paraffin should decrease with increasing projectile velocity when projectile masses are constant because the shear strength of paraffin increases with increased confining pressure. Although Palmer and others (1960) do not report a decrease in yield for their paraffin data, a decrease in yield for hypervelocity impact craters in Petroflex Plastic Wax (a petrolatum-paraffin mixture) with increased projectile velocities using constant projectile masses has been reported (Frasier, 1962, p. 374).

Normalized data for craters produced by hypervelocity impacts with basalt are about one order of magnitude larger than the corresponding normalized craters in copper, lead, aluminum, and water. This difference is caused by the spalling produced by tensile failure during reflection of stress waves from the free surface around the point of impact of rock targets (see, for example, Moore and others, 1962).

Conclusions

(1) Target strength is a more realistic parameter than target acoustic velocity for correlation of data on hypervelocity impact craters in the fluid-impact regime with those on low-velocity hydrodynamic or fluid-impact craters. The partial success obtained when using target acoustic velocity is probably the result of a close correlation between strength and acoustic velocity for certain materials (see for example, Maurer and Rinehart, 1960), but the correlation does not hold for water.

(2) The theory of Charters and Summers is approximately valid for craters produced by water drops impacting water and other craters in the fluid-impact regime.

(3) The dynamic strength of a material which yields under impact in the fluid-impact regime is greater than the strength at low confining pressure, and probably less than the product of the target density and heat of fusion, when significant amounts of vaporization of the target do not occur.

(4) The effects of target strength and target density at elevated confining pressures for craters in rocks and metals produced in the fluid-impact regime can be semiquantitatively estimated using the existing data at 49 kilobars. Strengths measured at this pressure not only give fair agreement between theory and experimental results with water-water impact, but also reduce the discrepancy between lead and copper experimental data when shear strengths at low confining pressures are used.

(5) Hypervelocity impact craters in rocks should be deeper than

corresponding craters in metals and water in the fluid-impact regime, because a projectile that has impacted rock is ejected along with debris, whereas one that has impacted metal smears out and plates the crater floors and walls.

(6) The volumes of hypervelocity impact craters in rocks should be larger than the corresponding volumes of craters in metals and water because of the spalling of the rock produced by tensile failure related to the reflections of stress waves from the free surfaces around the point of impact.

(7) More data on strengths at elevated confining pressures are needed in order to select proper parameters for correlation of hypervelocity impact data.

References cited

Al'tshuler, L. V., Kormer, S. B., Brazhnik, M. I., Vladimirov, L. A., Speranskaya, M. P., and Funtikov, A. I., 1960, The isentropic compressibility of aluminum, copper, lead, and iron at high pressures: Soviet Physics JETP, v. 11, p. 766-775.

Bridgman, P. W., 1935, Effects of high shearing stress combined with high hydrostatic pressure: Phys. Rev., v. 48, p. 825-847.

Chabai, A. J., and Hankins, D. M., 1960, Gravity scaling laws for explosion craters: U.S. Atomic Energy Comm., SC-4541 (RR), 18 p.

Charters, A. C., 1960, High speed impact: Sci. Am., v. 203, no. 4, p. 128-140.

Charters, A. C., and Summers, J. L., 1959, Some comments on the phenomena of high-speed impact, in Decennial symposium, May 26, 1959, White Oak U.S. Naval Ordnance Laboratory, Silver Spring, p. 1-21.

Engel, O. G., May 1961, Collisions of liquid drops with liquids: U.S. Nat. Bur. Standards Tech. Note 89, 30 p.

Frasier, J. T., 1962, Hypervelocity impact studies in wax: Symposium on hypervelocity impact, 5th, Denver 1961, Proc., v. 1, pt. 2, p. 371-388.

Halperson, S. M., and Atkins, W. W., 1962, Observations of hypervelocity impact: Symposium on hypervelocity impact, 5th, Denver 1961, Proc., v. 1, pt. 2, p. 497-509.

Lombard, D. B., 1961, The Hugoniot equation of state of rocks, in Symposium on rock mechanics, 4th, March 30, 31, and April 1, 1961, Proc.: Pennsylvania Min. Industries Expt. Sta. Bull. no. 76, p. 143-152.

Lyman, Taylor, ed., 1959, Metals handbook: Cleveland, Ohio, American Society for Metals, 1332 p.

Maurer, W. C., and Rinehart, J. S., 1960, Impact crater formation in rock: Jour. Appl. Physics, v. 31, p. 1247-1252.

Moore, H. J., and Gault, D. E., 1963, Relations between dimensions of impact craters and properties of rock targets and projectiles: U.S. Geol. Survey, Astrogeologic studies Annual progress report to NASA, August 25, 1961--August 24, 1962, pt. B, p. 38-79. Released to open file 5/15/63

Moore, H. J., Gault, D. E., and Lugn, R. V., 1962, Experimental hypervelocity impact craters in rock: Symposium on hypervelocity impact, 5th, Denver 1961, Proc., v. 1, pt. 2, p. 625-643.

Nordyke, M. D., 1962, An analysis of cratering data from desert alluvium: Jour. Geophys. Research, v. 67, p. 1965-1974.

Palmer, E. P., Grow, R. W., Johnson, D. K., and Turner, G. H., 1960, Cratering, experiment and theory: Symposium on hypervelocity impact, 4th, Eglin Air Force Base, Florida, 1960: U.S. Air Proving ground center APGC-TR-60-39, 17 p.

Rice, M. H., McQueen, R. G., and Walsh, J. M., 1948, Compression of solids by strong shock waves: Solid State Physics, v. 6, p. 1-63.

Robertson, E. C., 1955, Experimental study of the strength of rocks: Geol. Soc. America Bull., v. 66, p. 1275-1314.

Shoemaker, E. M., 1960, Penetration mechanics of high velocity meteorites, illustrated by Meteor Crater, Arizona: International Geol. Cong., 21st, Copenhagen 1960, pt. 18, p. 418-434.

Summers, J. L., 1959, Investigation of high speed impact--regions of impact and impact at oblique angles: U.S. Natl. Aeronautics and Space Admin. Tech. Note D-94, 18 p.

Whipple, F. L., 1958, The meteoritic risk to space vehicles, in Alperin Morton, Stern, Marvin, and Wooster, Harold, eds., Vistas in Astronautics, v. 1: New York, Pergamon Press, p.115-124.